Disks, Planetesimals, and Planets
ASP Conference Series, Vol. 219, 2000
F. Garzón, C. Eiroa, D. de Winter, and T. J. Mahoney, eds.

Circumbinary Disks around T Tauri stars: *HST*/NICMOS Near-Infrared Images and Polarimetric Maps

Gaspard Duchêne

Observatoire de Grenoble, Université Joseph Fourier, BP 53, 38041 Grenoble Cedex 9, France

Joel Silber

Department of Physical Sciences, University of Hertfordshire, College Lane, Hatfield, Hertfordshire AL10 9AB, UK

François Ménard

Canada–France–Hawaii Telescope Corporation, PO Box 1597, Kamuela HI 96743, USA

Tim Gledhill

Department of Physical Sciences, University of Hertfordshire, College Lane, Hatfield, Hertfordshire AL10 9AB, UK

Abstract. We have obtained new near-infrared images of both GG Tau and UY Aur circumbinary disks with the polarimetric modes of NICMOS aboard the *Hubble Space Telescope*. The 1 μm intensity map of GG Tau reveals a more complete elliptical shape than in previous ground-based images. Its eastern and western sides are definitely asymmetric. Our image strongly supports the ring geometry proposed by Guilloteau, Dutrey, & Simon (1999) on the basis of their millimeter interferometry images: a geometrically thick and sharply edged ring surrounding an empty gap around the binary. Around UY Aur, we identify structures that are in excellent agreement with the optical images of Ménard et al. (1999), which confirms that the inclination of the system to the line of sight is about 60 degrees. We also find tentative new structures closer to the stars.

1. Introduction

The presence of circumstellar disks around T Tauri stars has been suspected for a long time, but it is only very recently that these disks were directly detected, using high-angular millimeter imaging. These images revealed extended gas structures which appeared to be in Keplerian rotation around the central object. Among the rare detections so far, two disks were found around binary T Tauri stars: GG Tau (Dutrey, Guilloteau, & Simon 1994) and UY Aur (Duvert et al. 1998). The separations of the binaries are 0$''$.25 and 0$''$.89 respectively, which

correspond to projected physical separations of 35 and 125 AU at the distance of the Taurus star-forming region (140 pc).

In both cases, light scattered off the surface of the disks has been detected afterwards with adaptive optics imaging at near-infrared wavelengths. Roddier et al. (1996) found that the GG Tau ring has a clumpy appearance and that several radial spokes of material extend from the ring onto the central stars. The ring is brighter in its northern part, but is detected in all directions. They interpret this brightness difference as being due to the scattering geometry. The UY Aur case is very different, as Close et al. (1998) only detected the disk on one side of the binary. Furthermore, they found evidence that a "spiral arm" splits from the main disk and gets closer to the star. Deconvolution processes were applied in both studies to retrieve the highest spatial resolution allowed by adaptive-optics devices, and this may lead to some artifacts in the final images.

More recently, the first visible wavelength images of UY Aur were obtained by Ménard et al. (1999) at 600 and 800 nm with *HST*/WFPC2. The PSF-subtracted images revealed a more complicated structure that was found by Close et al. (1998): a large "clump" appears to be independent of the disk itself. If true, this implies that the inclination of the system to the line of sight is larger than was first thought (about 60° instead of about 40°).

To improve our knowledge of these two circumbinary disks, we have performed new observations at 1 μm and 2 μm of these systems with *HST*/NICMOS. We used the polarimetric modes, and we obtained both intensity and polarization maps, which do not need to be deconvolved. The GG Tau polarization maps are the first ever obtained of this system, while Potter et al. (1998) already presented a deconvolved J-band polarization map of UY Aur which revealed a nice centro-symmetric pattern. Polarization maps are powerful tools for investigating the dust-grain properties and the geometry and structure of the disks.

In Section 2, we summarize our observations and data processing steps, and the maps of both systems are presented and commented in Section 3. Section 4 describes some implications of our results on the properties of these disks.

2. Observations and Data Processing

The 1 μm and 2 μm images were obtained with Camera 1 and Camera 2 respectively, providing pixel scales of 0.″043 and 0.″075. Both binaries were observed through the three polarizers at each wavelength, during three 96 s exposures for each filter. The regular NICMOS data reduction pipeline proved to be unsatisfactory, and we had to re-reduce all the data, with particular care concerning the so-called "pedestal effect", to obtain final images where the sky level is flat all over the detector.

To allow clear detections of the disks, it is mandatory to remove the bright stellar point spread functions (PSFs). We first tried TinyTim PSFs, but it appeared that their match with the real ones is quite poor, so we turned to a "natural" star, i.e., a bright single star observed through the same filters. The diffraction-spike subtraction, though imperfect, is quite good, and the optical ghosts induced by some polarizers are naturally removed. Some residuals in the core of the PSFs, however, are still large, and nothing can be detected with certainty in the inner 0.″5 at 1 μm. At 2 μm, some fringing can be seen at

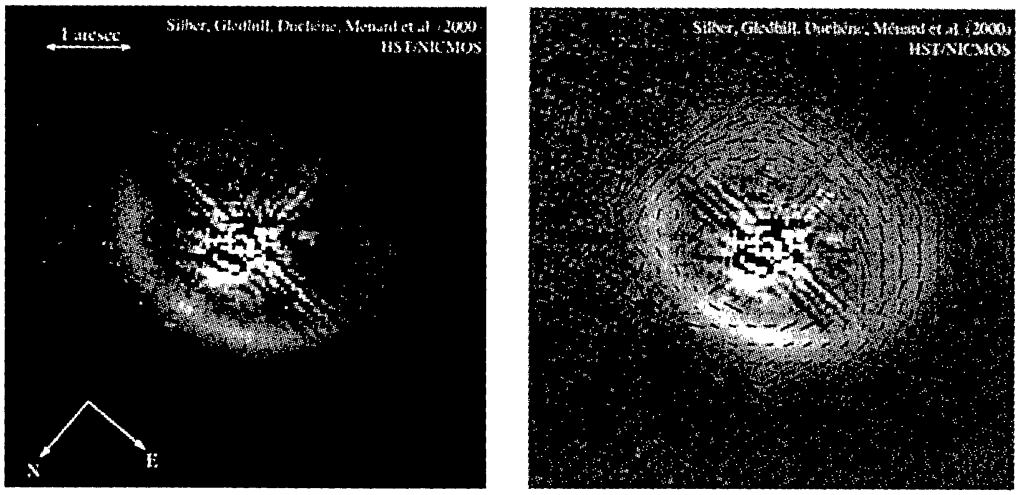

Figure 1. PSF-subtracted intensity (*left*) and polarization (*right*) maps of GG Tau at 1 μm.

separations as large as 3.″5. No deconvolution process was applied to our images, which allows an easier interpretation.

3. Results

3.1. GG Tau

The new 1 μm image of the GG Tau ring is presented in Figure 1. Its overall geometry is in good agreement with Roddier et al.'s (1996) images, though with a higher signal-to-noise ratio. However, there are some noticeable features. First, the ring does not appear clumpy in our image. This property was probably an artifact introduced by the deconvolution process applied to the adaptive-optics images. Fitting an ellipse to the ring, we find a semi-major axis, a position angle and an inclination in excellent agreement with the millimeter results of Guilloteau et al. (1999). It is noticeable, however, that this ellipse is not centered on the center of mass of the binary. Our image does not allow us to confirm the existence of the spokes of material discovered by Roddier et al. (1996), because of the large PSF-subtraction residuals inside the ring. Finally, a significant east–west asymetry in the northern part of the ring is seen in our intensity map.

The polarization vectors are strikingly well organized in a centro-symmetric pattern, which is symmetric about the semi-minor axis of the ring. The brightest part of the ring, which is closest to the observer, displays a lower polarization level than the faintest side, typically 20% as opposed to 50–60%.

At 2 μm, the disk is too close to the stars, and the large subtraction residuals prevent us from obtaining a clear image of the ring. However, we calculated the polarization map at this wavelength and, though the image is strongly dominated by the unpolarized stellar fluxes, a centro-symmetric pattern is found in the polarization vectors, with a typical level of 5–10%, indicating that the intrinsic polarization level of the light scattered by the ring is high.

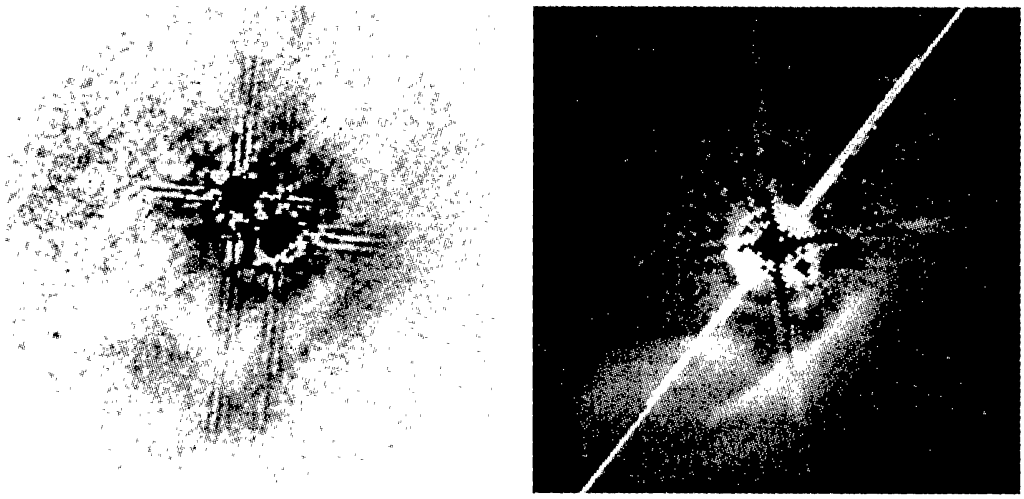

Figure 2. Intensity maps of UY Aur at 1 μm (this paper) and at 600 nm (from Ménard et al. 1999). Image sizes are 7.″7 and 12″, respectively. North is *up*, east to the *left*. The noisy area located to the east of the binary in the 1 μm image is due to a very low response of the detector.

3.2. UY Aur

The morphology of the UY Aur circumbinary disk in our new 1 μm image is in good agreement with Ménard et al.'s (1999) optical image, though the former suffer from a poor signal-to-noise ratio. As an be seen in Figure 2, the disk appears as an unresolved arc to the south-west of the binary at both wavelengths, while a bright clump to the south-east appears to be unrelated to this structure. Noticeably, the bright arc seems to widen to the west of the binary in our image. This can be interpreted as the arc breaking into two separate arcs: the disk itself remaining at least 2.″5 away from the stars, and an inner arc, getting closer to the stars. The latter would correspond to the "spiral arm" described by Close et al. (1998). A second feature in our map is an inner arc which is much brighter than the disk itself. It lies about 1″ to the south-west of the secondary. This may be a PSF artifact, but it can be seen using both a natural or a TinyTim-built PSF. Furthermore, its coincidence with a similar arc detected in the WFPC2 images is suggestive (see Figure 2). At 2 μm, the only area which is clearly separated from the PSF residuals is found to the south-east of the binary. It can be traced up to 5″ away from the stars. The back side of the disk remains undetected at both wavelengths, which provides strong constraints on the dust-grain properties. We note, however, that the small arc seen to the north-east of the primary at 1 μm can be seen in all individual images.

The polarization pattern at 2 μm is well organized in its south-eastern part, with all vectors well aligned, in a fashion consistent with centro-symmetry. The typical polarization level is about 40 per cent. At 1 μm, however, the picture is very different: though the vectors are basically aligned in the south-western part of the disk with a typical level of 20%, again in a more or less centro-symmetrical pattern, they are quite randomly oriented in the south-eastern clump. Whether this is due to our reduction pipeline, to the low signal-to-noise ratio, or reflects

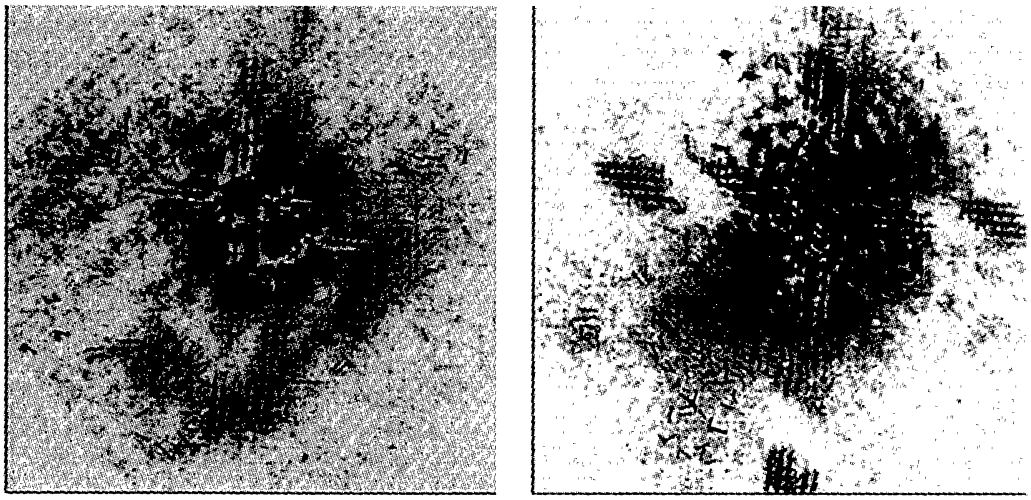

Figure 3. Polarization vectors superimposed on the intensity maps of UY Aur at 1 μm (*left*) and 2 μm (*right*). Image sizes are 7.″7 and 13″, respectively. Orientation of both images as in Figure 2.

the intrinsic pattern is unclear. It should be noted that Potter et al. (1998) found a very different behavior. Their data reduction process, however, included a deconvolution step, whose impact on the polarization is unknown.

4. Implications and Open Questions

4.1. GG Tau

As already pointed out by Guilloteau et al. (1999), the shift between the apparent center of the ring and the center of mass of the binary is naturally explained by a thick-ring geometry. This is related to the fact that, in Mie theory, forward scattering is strongly favored. Hence, most of the light scattered towards the observer comes from the upper part of the disk's inner edge, whose projection on the sky is not symmetric about the physical center of the ring. The quantitative model proposed by Guilloteau et al. (1999) is a ring with a half-thickness of 60 AU at its inner radius (180 AU) and a very sharp edge. The observed location of the ring appears to be in excellent agreement with the prediction from this model. Roddier et al. (1996) suggested that the thickness-to-radius ratio was about one tenth at the inner edge of the ring, which seems incompatible with our results.

The origin of the east–west asymetry is unclear. It may be due to the presence of two illuminating stars, or be related to the slight asymmetry found in the millimeter-wavelength image, which itself may reveal internal structures differences.

4.2. UY Aur

Fitting ellipses to the large south-western, unresolved arc both at 1μm and 600 nm yields very similar figures and, especially, an inclination to the line of sight of about 60° in both cases. This is much larger than the 42° estimated by Close

et al. (1998). The reason for that discrepancy is that they assumed that the south-east clump belongs to the disk, which now seems unlikely. Duvert et al. (1998) pointed out that a larger inclination (60–70°) is in better agreement with the millimeter observations.

If the inner arc close to the secondary star proves to be real, it will represent a challenge for theoretical studies, as most of these predict that structures at such a location should be highly unstable due to interaction with the binary system.

4.3. Monte Carlo Modeling

The polarization levels, as well as the front-to-back side flux ratios, are tightly linked to the disk geometry and to the dust grain properties. Our next step in this study is to run Monte Carlo simulations to investigate these properties. For instance, we may determine whether the dust-grain size distribution in the disks is compatible with that of interstellar grains. In principle, we will also constrain the amount of "flaring" in both disks, as well as their geometrical height and optical depth.

References

Close, L., Dutrey, A., Roddier, F., Guilloteau, S., Roddier, C., Northcott, M., Ménard, F., Duvert, G., Graves, J., & Potter, D. 1998, ApJ, 499, 833

Dutrey, A., Guilloteau, S., & Simon, M. 1994, A&A, 286, 149

Duvert, G., Dutrey, A., Guilloteau, S., Ménard, F., Schuster, K., Prato, L., & Simon, M. 1998, A&A, 332, 867

Guilloteau, S., Dutrey, A., & Simon, M. 1999, A&A, 348, 570

Ménard, F., Stapelfeldt, K., Krist, J., Duvert, G., Padgett, D., & Burrows, C. 1999, BAAS, 194, 6811

Potter, D., Close, L., Roddier, F., Roddier, C., Graves, J., & Northcott, M. 1998, in ESO Conf proceedings, 56, Astronomy with Adaptive Optics, ed. D. Bonaccini (Garching: ESO), p. 353

Roddier, C., Roddier, F., Northcott, M., Graves, J., & Jim, K. 1996, ApJ, 463, 326